Hidden Life In The Bands: Analyzing Hofstadter's Butterfly

Shrikar Dulam[1], Sarah Wang[2], Hyeonsu Kang[3], and Juwon Bae[3]

[1]University of Illinois Urbana-Champaign
[2]Massachusetts Institute of Technology
[3]Kyung Hee University

August 6, 2025

Abstract

Hofstadter's butterfly is a striking fractal pattern that emerges when electrons move through a two-dimensional lattice in the presence of a magnetic field, revealing deep connections between quantum mechanics, band structure, and topology. In this project, we explore the rich structure of the energy spectrum using Python. By numerically diagonalizing the system's Hamiltonian, we computed the allowed energy levels for electrons under varying magnetic flux. To study the topological nature of these energy bands, we applied the Diophantine equation developed by TKNN to calculate the Chern numbers, which relate directly to the quantized Hall conductance observed in the quantum Hall effect. We extended our analysis beyond the standard square lattice to include a hexagonal (graphene-like) lattice structure, comparing how lattice geometry affects the spectrum. Finally, we created animations to visualize the fractal nature of the butterfly.

1 Introduction

Understanding how electrons behave within crystalline solids is a fundamental goal of condensed matter physics. In such systems, the periodic potential arising from the atomic lattice leads to the formation of energy bands which characterize useful properties of the material. For example, the band structure can help classify materials as a conductor, insulator, or semiconductor.

However, applying a magnetic field drastically changes the electronic behavior, as observed with the integer quantum Hall effect. Discovered in 1980, it was shown that the Hall conductance of a two-dimensional electron gas was found to be quantized in integer multiples of $e^2/c\hbar$ [1]. Specifically, the quantized Hall conductance was shown to correspond to a topological invariant known as the Chern number. This novel intersection of topology and condensed matter has paved the way for robust electronic devices, topological quantum computing, and new quantum materials [2, 3].

Douglas Hofstadter began exploring this crossroad of subjects with a tight-binding model on a two-dimensional square lattice, with a uniform magnetic field perpendicular to the plane. By numerically computing the energy spectrum as a function of the magnetic flux per unit cell, he discovered that the resulting plot formed a self-similar, recursive pattern that later became known as Hofstadter's Butterfly [4].

In this project, we seek to understand the underlying physics of the beautiful butterfly. We first derive the model Hamiltonian from the ground up. Then, we briefly describe the topological properties, including its Chern numbers and Hall conductivities, and the key aspects of our Python program to analyze this system. We conclude with visuals showcasing the major results and an appendix for further elaboration.

2 Theory

2.1 Hamiltonian Model

At a high level, an ordinary lattice enforces spatial symmetry that allows electrons to form Bloch states and move through the crystal in energy bands. However, the magnetic field curves the paths of the electrons, opposing the crystal symmetry. The magnetic field ultimately reconciles with the lattice symmetry through additional quantum phase shifts in the electron's wavefunction as it hops from site to site [5].

Quantitatively, we can first derive the energy dispersion relation in a square lattice without any magnetic field by first applying Bloch's theorem to constrain the form of the electron wavefunction within the lattice. Applying the tight-binding principle and the linear combination of atomic orbitals yields the following:

$$E(k) = \epsilon - 2t(\cos(k_x a) + \cos(k_y a))$$

Now, we can begin to derive an effective Hamiltonian by converting the energy dispersion into an operator [4]. The key step in the derivation is the Peierls substitution, in which we introduce a kinetic momentum term that accounts for the effect of the magnetic field [5]. It is further discussed in the appendix 5.2.

$$\epsilon - 2t\left(\cos\left(\frac{p_x - \frac{e}{c}A_x}{\hbar}a\right) + \cos\left(\frac{p_y - \frac{e}{c}A_y}{\hbar}a\right)\right)$$

The magnetic vector potential is given by A:

$$B = \nabla \times A$$

However, A is not unique, as we can always add a gradient to A. This means we can choose a convenient form of A, known as a gauge. We choose the Landau gauge:

$$A = (0, Bx, 0)$$

This simplifies our calculations since this gauge only adds phase when hopping in the y-direction [6].

Now, we convert our scalar equation for energies into operator form for wavefunctions. We use the canonical substitution $\vec{p} \to -i\hbar\nabla$

$$\epsilon - 2t\left(\cos\left(-ia\frac{\partial}{\partial x}\right) + \cos\left(\frac{-i\hbar\frac{\partial}{\partial y} - \frac{e}{c}Bx}{\hbar}a\right)\right)$$

Decomposing the cosines into exponential form using Euler's formula, we get:

$$\hat{H}_{\text{eff}} = \epsilon - t\left(e^{a\frac{\partial}{\partial x}} + e^{-a\frac{\partial}{\partial x}} + e^{\frac{-ie}{\hbar c}Bxa}\cdot e^{a\frac{\partial}{\partial y}} + e^{\frac{ie}{\hbar c}Bxa}\cdot e^{-a\frac{\partial}{\partial y}}\right)$$

Each exponential represents a translation operation: $\psi(x) \to \psi(x \pm a)$. When we apply this operator to Schrödinger's equation, we get:

$$\psi(x+a,y)+\psi(x-a,y) + \exp\left(\frac{-ie}{\hbar c}Bxa\right)\psi(x,y+a) + \exp\left(\frac{ie}{\hbar c}Bxa\right)\psi(x,y-a) = \frac{E-\epsilon}{t}\psi(x,y)$$

We can now parameterize the constants related to energy and magnetic field: $\epsilon_0 = \frac{E-\epsilon}{t}, \alpha = \frac{a^2 B}{hc/e}$.

We also express distance in terms of discrete lattice length multiples $x = ma, y = na$ yielding:

$$\psi_{m+1,n}+\psi_{m-1,n} + \exp\left(-2\pi i\alpha m\right)\psi_{m,n+1} + \exp\left(2\pi i\alpha m\right)\psi_{m,n-1} = \epsilon_0\psi_{m,n}$$

We then assume separation of variables and supply a nice ansatz:

$$\psi_{m,n} = e^{i\upsilon n} g_m$$

Which factorizes the wavefunction into a plane-wave along the y-direction whose amplitude varies along x. This yields:

$$\psi_{m+1,n} + \psi_{m-1,n} = (\epsilon_0 - (e^{i(\upsilon - 2\pi\alpha m)} + e^{-i(\upsilon - 2\pi\alpha m)}))\psi_{m,n}$$

or the Harper Equation [5].

$$\psi_{m+1} + \psi_{m-1} = (\epsilon_0 - 2\cos(\upsilon - 2\pi\alpha m))\psi_m$$

2.2 Topological Properties

It can be convenient to convert from the real space positions of the lattice to a momentum-based space known as the Brillouin zone. This mapping can be done through Fourier transform, and it turns out that the Brillouin zone is a 2-torus. This nontrivial topological structure constrains wavefunctions on momentum space as they must be well defined when you translate them a cycle around on the torus. Additionally, the wavefunction picks up a Berry phase as it travels around the torus, which can be analogous to the wavefunction "twisting" around due to geometry. We can compute the net effect of the Berry phase by integrating the Berry curvature over the entire Brillouin zone, yielding the Chern number [7].

The torus topology then forces the Chern number to be quantized, and it can be shown that the Hall conductance subsequently becomes quantized as well when averaging the flux [7]. Since the Chern number cannot change continuously, the Hall conductivity is robust to deformation in the system. Thus, we can see how topological properties have a crucial impact on the lattice behavior.

To understand how these topological features manifest in a lattice under a magnetic field, we must consider the magnetic Brillouin zone, which arises when the magnetic flux through a unit cell is a rational multiple of the flux quantum, $\Phi/\Phi_0 = p/q$. In this case, the presence of the magnetic field enlarges the unit cell, effectively folding the original Brillouin zone into q subbands. Each of these bands can carry a distinct Chern number, and the sum of their contributions determines the total Hall conductance [7].

3 Computational Details

We primarily used basic Python libraries like NumPy and Pandas for data manipulation, Scipy for matrix diagonalization via scipy.linalg.eigh(), and Matplotlib for visuals. For the sake of modularity, we split up the functions such that one function computes pertinent data like energy spectrum and Chern numbers while another function plots the data. The code is commented and organized into different categories like generating static graphs, plotting topological data, and producing animations.

To obtain energy spectrums, we revisit the Harper equation, which we can convert into proper system of equations in matrix form:

$$\begin{pmatrix} \psi_{m+1} \\ \psi_m \end{pmatrix} = \begin{pmatrix} \epsilon_0 - 2\cos(2\pi\alpha m - \upsilon) & -1 \\ 1 & 0 \end{pmatrix} \begin{pmatrix} \psi_m \\ \psi_{m-1} \end{pmatrix}$$

This matrix is known as a transfer matrix as it propagates the wavefunction forward in position. When $\alpha = \frac{p}{q}$, we can impose periodic boundary conditions $\psi_{m+q} = \psi_q$, so we can multiply q transfer matrices together to get the monodromy matrix M. We can ensure the wavefunction is well-behaved with the trace condition $|Tr(M)| \leq 2$, so we can just iterate through all possible energies to see which are allowed [4]. This energy iteration approach can be fruitful for computing Lyapunov exponents as well, but it is computationally taxing to get a good resolution with the graph. Thus, this method is neglected in favor of direct diagonalization for the full spectrum of energies.

We can construct the full finite difference matrix as follows:

$$H_q\psi = \begin{pmatrix} V_0 & 1 & 0 & \dots & e^{-ikq} \\ 1 & V_1 & 1 & \dots & 0 \\ 0 & \ddots & \ddots & \ddots & \vdots \\ \vdots & & 1 & V_{q-2} & 1 \\ e^{ikq} & & & 1 & V_{q-1} \end{pmatrix} \begin{pmatrix} \psi_0 \\ \psi_1 \\ \vdots \\ \psi_{q-2} \\ \psi_{q-1} \end{pmatrix}$$

For further explanation of the Harper matrix, see 5.3.

We also compute the spectrum for a hexagonal lattice derived from Rammal's work [8]. In particular, the finite difference matrix can be derived with the equation:

$$\begin{aligned} \lambda\psi_m = &\ 2\cos\left[-\pi\frac{p}{q}\left(m+\frac{1}{2}\right)+\kappa\right]\psi_{m+1} \\ &+ 2\cos\left[-\pi\frac{p}{q}\left(m-\frac{1}{2}\right)+\kappa\right]\psi_{m-1} \\ &+ 2\cos\left[-2\pi\frac{p}{q}\left(m+\frac{1}{2}\right)+2\kappa\right] \end{aligned}$$

Where $\lambda = \epsilon^2 - 3, \kappa = k_y a\frac{\sqrt{3}}{2}$.

While we could calculate Chern numbers for the butterfly by numerically integrating the Berry curvature over the magnetic Brillouin zone, there is a simpler number-theoretic method developed by Thouless, Kohomoto, Nightingale and den Nijs [4]. When the magnetic flux is rational $\Phi/\Phi_0 = p/q$, we can solve the linear Diophantine equation:

$$r = qs_r + pt_r$$

Where $|t_r| \leq q/2$. The Chern number of the r^{th} band out of the q bands present is then

$$C = t_r - t_{r-1}$$

Where $t_0 \equiv 0$. The Hall conductivity when the r bands are filled ($E_r < E_f < E_{r+1}$) then becomes:

$$\sigma_{xy} = \frac{e^2}{2\pi\hbar}t_r$$

We then computed the quantized Hall conductance for each gap by summing over the filled bands below.

4 Results

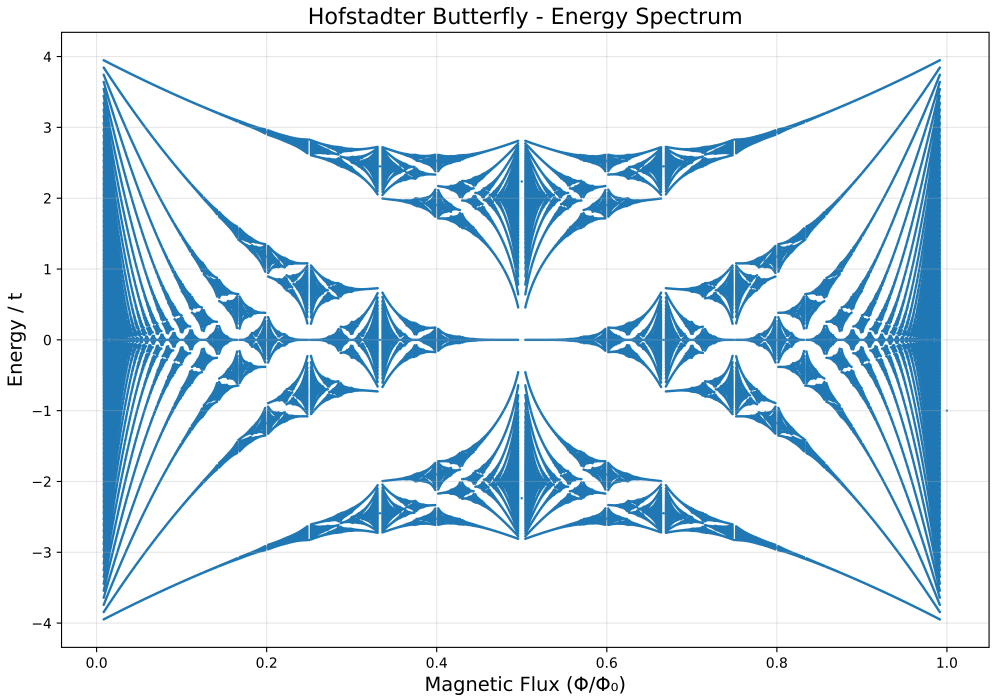

Figure 1: The Hofstadter butterfly energy spectrum for the two-dimensional square lattice. The horizontal axis shows the dimensionless magnetic flux per unit cell, $\alpha = \Phi/\Phi_0$, computed for rational values $\alpha = p/q$ with denominators up to $q = 120$. The vertical axis shows the allowed energy levels for an electron on a 2D lattice under a perpendicular magnetic field. The fractal structure reveals the splitting of energy bands as magnetic and lattice periodicities compete. We note the quadratic band edges at $E = \pm 4t$.

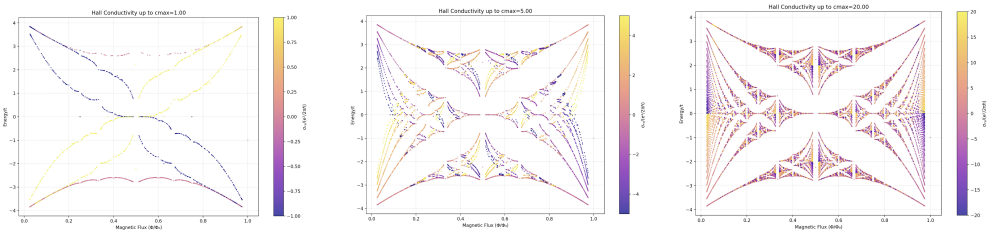

(a) $|\sigma_{xy}| \leq 1$ (b) $|\sigma_{xy}| \leq 5$ (c) $|\sigma_{xy}| \leq 20$

Figure 2: Filtered Hofstadter butterfly highlighting topological phases with increasing Hall conductivity bounds. Each panel displays the energy spectrum bounded by an absolute Hall conductivity $|\sigma_{xy}| = n$. As n grows, finer features of the fractal structure emerge, revealing the hierarchical organization of topological phases labeled by Chern numbers.

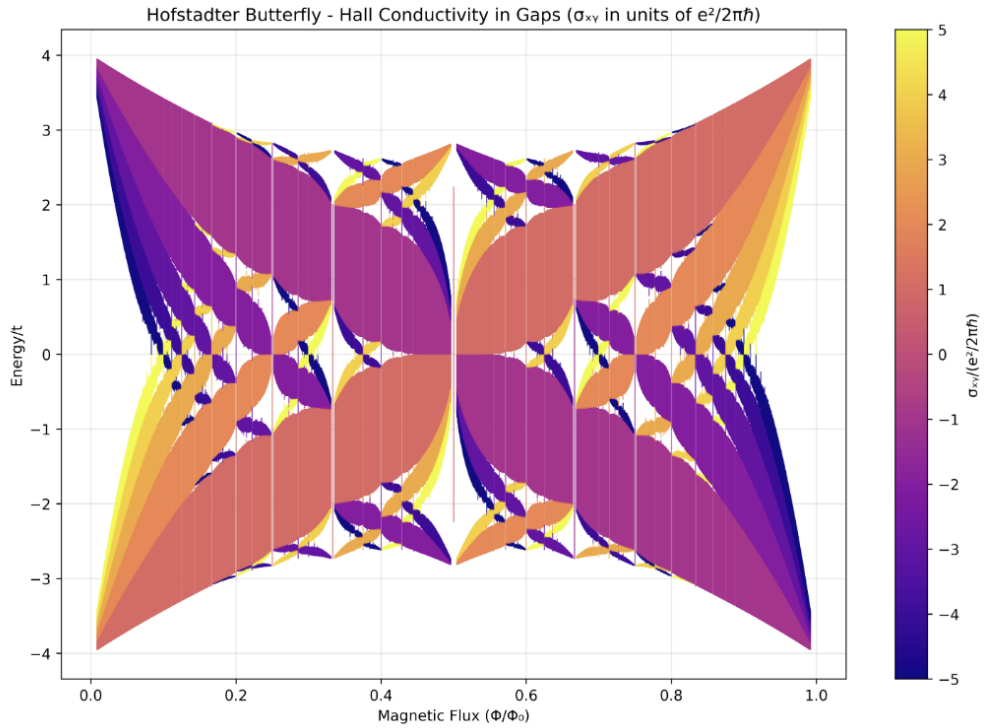

Figure 3: A topological phase diagram of the Hofstadter butterfly based on the quantized Hall conductivities of each region. There are infinite phases present, but for visual clarity, only regions $\sigma_{xy} \leq 5$ are colored. This result faithfully reproduces the diagram in Satija's paper [9].

.

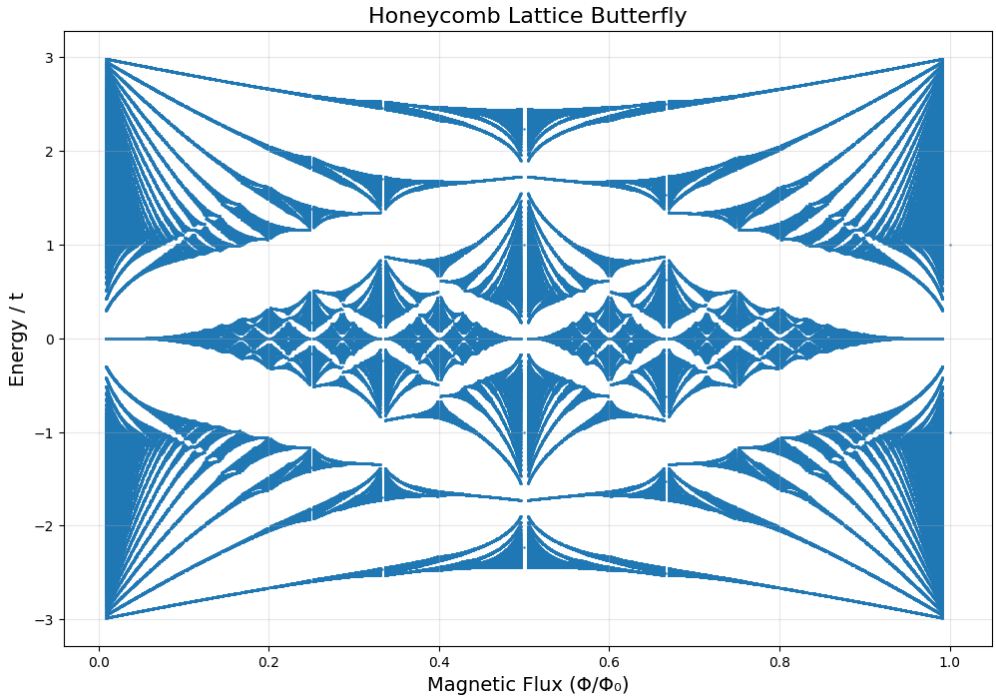

Figure 4: The Hofstadter butterfly spectrum for a honeycomb lattice. Unlike the square lattice case with uniform bands and quadratic edges, the central Dirac point at zero flux evolves into relativistic minibands, and the spectrum reflects the two-sublattice structure with more complex gap patterns and sharper band edges at $E = \pm 3t$. The result was derived from Rammal's work [8].

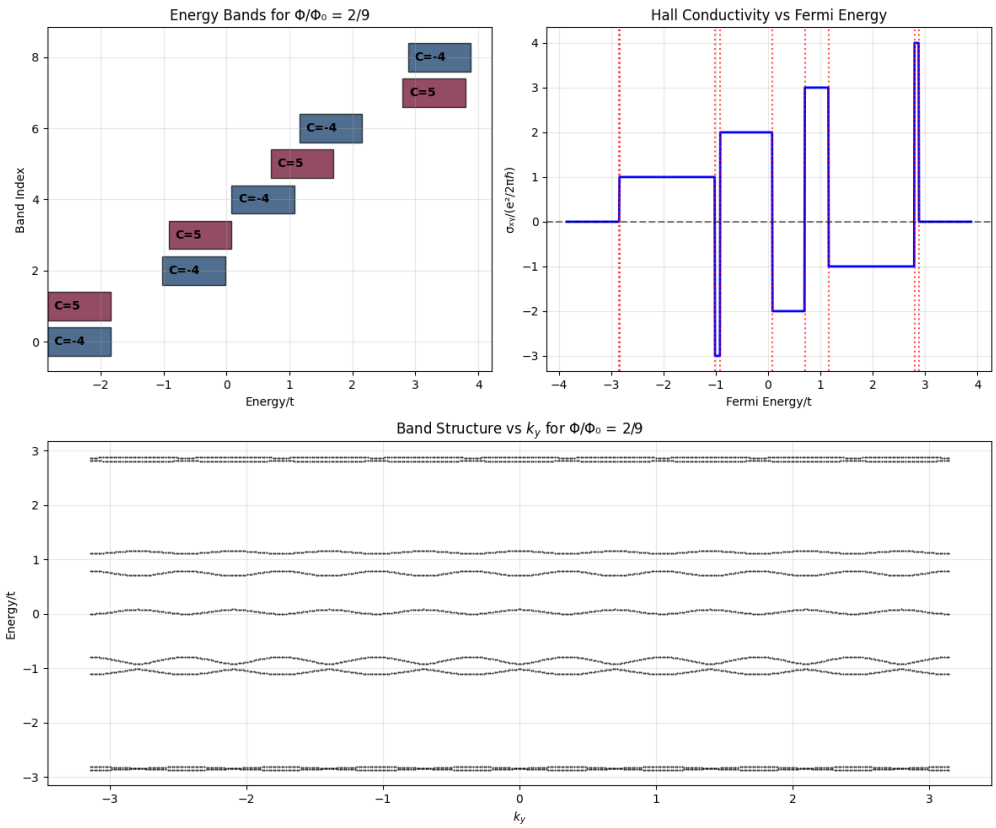

Figure 5: A detailed analysis of the Hofstadter spectrum at magnetic flux $\alpha = 2/9$. As predicted, the periodicity of the magnetic flux leads to the formation of $q = 9$ energy bands, shown in the top-left plot, each labeled with its corresponding Chern number. The alternating sequence of topological invariants reflects the nontrivial band topology. The top-right plot shows the quantized Hall conductivity changing nontrivially as the Fermi energy crosses each gap. The bottom plot shows the band dispersion along the y-direction, illustrating the weak dependence on momentum and revealing how narrow or broad each band is. Together, these panels highlight how magnetic field-induced band splitting and topological classification govern transport behavior in the system.

5 Appendix

5.1 Bloch's Theorem

Bloch's theorem applies to electrons within a 2D lattice. It says that a valid wavefunction for an electron can be decomposed into two parts: a function that has the same period as the lattice and a plane wave.

$$\psi(\mathbf{x}) = u_{\mathbf{k}}(\mathbf{x})\exp(i\mathbf{k}\cdot\mathbf{x})$$

Our goal is to show that any valid wavefunction for a periodic potential can be decomposed in this way.

To do this, we first show that the translation and energy operators commute [10]. It is known that if operators commute, they will share some eigenstates. The eigenstates we care about are the ones that they share.

$$\begin{aligned}\hat{T}(\mathbf{R})\hat{H}(\mathbf{x})\psi(\mathbf{x}) &= \hat{H}(\mathbf{x}+\mathbf{R})\psi(\mathbf{x}+\mathbf{R}) \\ &= \hat{H}(\mathbf{x})\psi(\mathbf{x}+\mathbf{R}) \\ &= \hat{H}(\mathbf{x})\hat{T}(\mathbf{R})\psi(\mathbf{x})\end{aligned}$$

We assume that Hamiltonian is invariant under translations by lattice length. Under this assumption, the operators commute. Now we find properties of the translation operator's eigenvalues:

$$\hat{T}(\mathbf{R})\psi(\mathbf{x}) = c(\mathbf{R})\psi(\mathbf{x})$$

We have the constraint that $c(\mathbf{R})$ must be a phase factor, since translation shouldn't change the total probability given by the wavefunction. Second, $c(\mathbf{R})$ must reflect how translations work, namely that $c(\mathbf{a}+\mathbf{b}) = c(\mathbf{a})c(\mathbf{b})$.

The first condition limits $c(\mathbf{R})$ to the form $e^{i\theta}$. The second condition limits it to be such that $c(\mathbf{R}) = e^{i\mathbf{k}\cdot\mathbf{R}}$, where k is the wavevector. This means that the translation operator corresponds to a phase factor.

Now we define a new function that we hope to show is periodic.

$$u_k(\mathbf{x}) := \exp(-i\mathbf{k}\cdot\mathbf{x})\psi(\mathbf{x})$$

Applying a translation, we get that u_k is lattice periodic:

$$\begin{aligned}u_k(\mathbf{x}+\mathbf{R}) &= \exp(-i\mathbf{k}\cdot\mathbf{x})\exp(-i\mathbf{k}\cdot\mathbf{R})\psi(\mathbf{x}+\mathbf{R}) \\ &= \exp(-i\mathbf{k}\cdot\mathbf{x})\psi(\mathbf{x}) \\ &= u_k(\mathbf{x})\end{aligned}$$

We showed that $u_k(x)$ is periodic. Since u_k was just a function definition that used ψ, it means that for any ψ, we can write it in a periodic function multiplied by a phase factor.

We have thus proven our original claim that we can decompose the wavefunction in such a way:

$$\psi(\mathbf{x}) = u_{\mathbf{k}}(\mathbf{x})\exp(i\mathbf{k}\cdot\mathbf{x})$$

where we can think of u_k as some initially unknown periodic function.

We employ Bloch's theorem in calculating the energy dispersion for a 2D crystal, which is the starting point for Hofstadter's butterfly. For a derivation, see [11].

5.2 Intuition for Peierls Substitution

In our derivation of $\hat{H}_{\text{eff}}$, we apply the Peierls substitution to account for electromagnetic effects on the tight binding model.

In the presence of electromagnetic fields, the kinetic momentum (what appears in the Schrödinger equation) becomes $p - eA$ instead of just p [12].

This originates from Lagrangian mechanics. The Lagrangian for a charged particle is given by

$$L = 1/2m\mathbf{v}^2 - e\Phi + e(x \cdot \mathbf{A})$$

The canonical momentum is given as

$$\mathbf{p}_{\text{canonical}} = \frac{\partial L}{\partial \mathbf{v}} = m\mathbf{v} + q\mathbf{A}$$

where $\mathbf{A}$ is the vector potential. The kinetic momentum is then

$$\mathbf{p}_{\text{kinetic}} = m\mathbf{v} = \mathbf{p}_{\text{canonical}} - q\mathbf{A}$$

The key step in Peirels substitution is substituting crystal momentum $\hbar k$ for kinetic momentum. Then, we promote momentum to its operator form.

The Hamiltonian in the Schrödinger equation uses the kinetic momentum operator $\hat{\mathbf{p}}_{\text{kinetic}} = \hat{\mathbf{p}} - q\mathbf{A}$, where $\hat{\mathbf{p}} = -i\hbar\nabla$ is the canonical momentum operator. Using the Landau gauge, we get $A = (0, Bx, 0)$, whose values we use for the qA term.

The physical validity of this substitution for quantum lattice systems has been extensively analyzed and justified [13, 14].

5.3 Harper matrix

Recall the Harper equation

$$\psi_{m+1} + \psi_{m-1} = (\epsilon - 2\cos(2\pi\alpha m - \phi))\psi_m \tag{1}$$

and the resulting Harper matrix:

$$H_q\psi = \begin{pmatrix} V_0 & 1 & 0 & \cdots & e^{-ikq} \\ 1 & V_1 & 1 & \cdots & 0 \\ 0 & \ddots & \ddots & \ddots & \vdots \\ \vdots & \cdots & 1 & V_{q-2} & 1 \\ e^{ikq} & 0 & \cdots & 1 & V_{q-1} \end{pmatrix} \begin{pmatrix} \psi_0 \\ \psi_1 \\ \vdots \\ \psi_{q-2} \\ \psi_{q-1} \end{pmatrix} = \epsilon \begin{pmatrix} \psi_0 \\ \psi_1 \\ \vdots \\ \psi_{q-2} \\ \psi_{q-1} \end{pmatrix} \tag{2}$$

where $V_m = 2\cos(2\pi\alpha m - \phi)$ represents the diagonal potential terms.

The off-diagonal corner elements $e^{\pm ikq}$ arise from the periodic boundary conditions imposed by Bloch's theorem. Since we require $\psi_{m+q} = e^{ikq}\psi_m$, the contribution to ψ_0 from ψ_{-1} can be written as $e^{-ikq}\psi_{q-1}$, and similarly for the opposite corner.

References

[1] Klaus von Klitzing. The quantized hall effect. *Rev. Mod. Phys.*, 58:519–531, Jul 1986.

[2] Joel E Moore. The birth of topological insulators. *Nature*, 464(7286):194–198, 2010.

[3] Filippo Iulianelli, Sung Kim, Joshua Sussan, and Aaron D Lauda. Universal quantum computation using ising anyons from a non-semisimple topological quantum field theory. *arXiv preprint arXiv:2410.14860*, 2024.

[4] Douglas R. Hofstadter. Energy levels and wave functions of bloch electrons in rational and irrational magnetic fields. *Phys. Rev. B*, 14:2239–2249, Sep 1976.

[5] R. Peierls. *On the Theory of the Diamagnetism of Conduction Electrons*, pages 97–120.

[6] LD Landau. Diamagnetismus der metalle. *Zeitschrift für Physik*, 64(9):629–637, 1930.

[7] David Tong. Lecture notes on the quantum hall effect: "the integer quantum hall effect". Lecture notes, DAMTP, University of Cambridge, 2016. Section 2: "The Integer Quantum Hall Effect".

[8] Rammal, R. Landau level spectrum of bloch electrons in a honeycomb lattice. *J. Phys. France*, 46(8):1345–1354, 1985.

[9] Indubala Satija. Pythagorean triplets, integral apollonians and the hofstadter butterfly, 2018.

[10] University of Stuggart. *Chapter 3: Electrons in a periodic potential.*

[11] Mervyn Roy. The tight binding model, 2015.

[12] David Tong. Applications of quantum mechanics university of cambridge part ii mathematical tripos. Lecture notes, DAMTP, University of Cambridge, 2016. Chapter 6: "Particles in a Magnetic Field".

[13] J. M. Luttinger. The effect of a magnetic field on electrons in a periodic potential. *Phys. Rev.*, 84:814–817, Nov 1951.

[14] Walter Kohn. Theory of bloch electrons in a magnetic field: The effective hamiltonian. *Phys. Rev.*, 115:1460–1478, Sep 1959.